Reactions of Imidazolio-Phosphides with Organotin Chlorides : Surprisingly Diverse

Goerigk, Florian

2022-03-18

Goerigk , F , Birchall , N , Feil , C M , Nieger , M & Gudat , D 2022 , ' Reactions of Imidazolio-Phosphides with Organotin Chlorides : Surprisingly Diverse ' , European Journal of Inorganic Chemistry , vol. 2022 , no. 8 , 202101026 . https://doi.org/10.1002/ejic.202101026

http://hdl.handle.net/10138/350911
https://doi.org/10.1002/ejic.202101026

EurJIC
European Journal of Inorganic Chemistry

Research Article
doi.org/10.1002/ejic.202101026

Chemistry Europe
European Chemical Societies Publishing

www.eurjic.org

Reactions of Imidazolio-Phosphides with Organotin Chlorides: Surprisingly Diverse

Florian Goerigk,[a] Nicholas Birchall,[a] Christoph M. Feil,[a] Martin Nieger,[b] and Dietrich Gudat*[a]

Dedicated to Professor Dr. Frank Uhlig on the occasion of his 60th birthday.

Reactions of primary imidazolio-phosphides ("imidazolylidene-phosphinidenes") with R_2SnCl_2 yield as main products spectroscopically detectable Lewis pairs which undergo base-induced dehydrochlorination in the presence of excess dichlorostannane to afford zwitterionic chloride adducts of distannylated imidazolio-phosphines. In contrast, reactions with R_3SnCl proceed under dismutation to furnish mixtures containing imidazolium salts and stannylated (oligo)phosphines $P(SnR_3)_3$ and $P_7(SnR_3)_3$, respectively. DFT studies were used to rationalize the divergent behavior based on the presumption that the reactions proceed under thermodynamic control and the products observed represent the most stable species under the specific reaction conditions. Computational simulation of selected reaction steps provides a model mechanism for Lewis-acid promoted creation of PP-bonds, which is a prerequisite for oligophosphine formation. The computational studies further highlight parallels between reactions of imidazolio-phosphides with Lewis and Brønsted acids, and allow also to extrapolate the behavior of the P-nucleophiles towards other electrophiles than organotin chlorides.

Introduction

Nominal primary imidazolylidene-phosphinidenes **A**[1–4] have caught attention because of their multifaceted reactivity towards Brønsted acids and electrophiles.[5] Depending on the conditions, **A** may react via attachment of an electrophile to produce cationic phosphines **B**,[6–7] via P–H bond functionalization to afford substitution products **C**,[3,7–9] or via condensation under cleavage of an imidazolium salt to furnish cyclic oligophosphines **D**,[7] respectively (Scheme 1). This varied reactivity can be rationalized in the framework of a valence bond description invoking canonical formulae **A'**–**A'''** as principal resonance structures.[5,10] The contributions of the polar structures **A''**, **A'''** imply a significant P-nucleophilic character that is encountered in all molecules with a C,C-diamino-substituted phosphorus-carbon double bond and led to their categorization as "inversely polarized" phosphaalkenes.[11] This nucleophilicity enables **A** to yield neutral adducts with one or even two transition metal or main group element-based Lewis acids,[5,6,12]

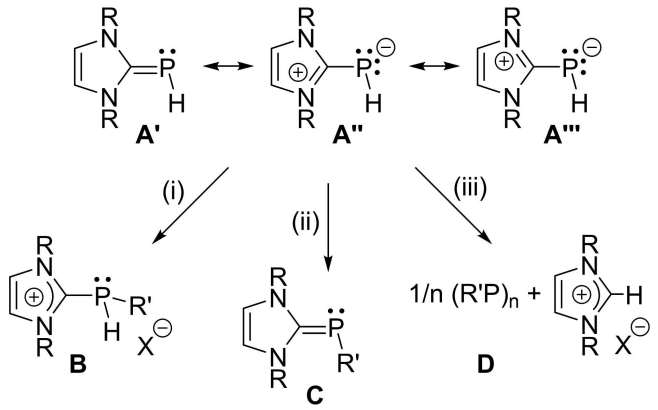

Scheme 1. Molecular structure and fundamental reactions of primary imidazolio-phosphides A. Reagents: (i) + R'X (R' = H, alkyl); (ii) a) + R'X, b) + base, – base·HX (R' = alkyl, phosphinyl); (iii) + R'X, base catalyst (R' = H, alkyl).

respectively, and provides also a strong driving force for the formation of cations **B**. The cations are then intermediates in the generation of **C** and **D** by alkylation/deprotonation or autocatalytic cascades of alkylation and intermolecular condensation steps.[7]

Because their reactions reflect typical reactivity patterns of phosphides R_2P^-, we suggested addressing compounds **A** as zwitterionic imidazolio-phosphides.[7] This view is also in accord with the fact that a typical double bond reactivity of **A** is largely unknown, indicating that phosphaalkene structure **A'** (identified as the leading resonance structure in the description of parent **A**[10]) appears to have little impact on the chemical behavior.

Given that functionalization of primary imidazolio-phosphides through base-induced PH-bond metathesis is not

[a] F. Goerigk, N. Birchall, Dr. C. M. Feil, Dr. D. Gudat
Institut für Anorganische Chemie
Universität Stuttgart
Pfaffenwaldring 55, 70550 Stuttgart, Germany
E-mail: gudat@iac.uni-stuttgart.de
https://www.iac.uni-stuttgart.de/forschung/akgudat/
[b] Dr. M. Nieger
Department of Chemistry
University of Helsinki
P.O Box 55, 00014 University of Helsinki, Finland

Supporting information for this article is available on the WWW under https://doi.org/10.1002/ejic.202101026

Research Article
doi.org/10.1002/ejic.202101026

confined to alkylation but enables the introduction of phosphinyl groups[3,9] or mercuration,[13] we began to explore the reactivity of **A** towards an extended range of electrophiles. Here, we report on reactions with organotin chlorides, which reveal an unexpected and quite diverse behavior of the phosphorus nucleophiles.

Results and Discussion

The only synthesis of a P-stannylated imidazolio-phosphide reported to date was accomplished by reacting phosphaketene $Ph_3Sn–P{=}C{=}O$ with an N-heterocyclic carbene.[14] Introduction of a tin-containing substituent by post-functionalization of a PH-substituted precursor has precedence in the preparation of a stannylated dihydroimidazolio-phosphide with a C-saturated heterocycle.[15] However, the applied protocol entailing metalation of the PH-bond and subsequent salt metathesis with an organotin dichloride seems unamenable to imidazolio-derivatives **A** as the PH-bond is here effectively protected by the enhanced acidity of the CH-bonds at the imidazole ring, which redirects the attack of the metalating agent to the heterocycle.[16]

Anticipating that the alkylation-deprotonation approach used to introduce alkyl or phosphinyl groups[3,7–9] would allow to avoid this obstacle, we studied the reactions of imidazolio-phosphides **1a,b** with Me_3SnCl and Ph_3SnCl in the presence of tertiary amines. To our surprise, we did not obtain any evidence of the expected substitution products, but observed the formation of mixtures containing substantial amounts of soluble imidazolium salts [**2a,b**]Cl and intractable precipitates previously recognized as insoluble polyphosphorus species.[7] ^{31}P NMR studies disclosed that tristannyl phosphine **3**[17] was formed as main[18] or even only detectable soluble phosphorus-containing product with Ph_3SnCl (Scheme 2) while both **4**[19] and tristannyl heptaphosphine **5**[20] were established as the products of the reaction of **1a** with Me_3SnCl. Remarkably, the reactions proceeded in the same way, but even more cleanly, when the tertiary amine was omitted.

Having noticed that the successful stannylation of a metalated dihydroimidazolio-phosphide had in fact been carried out with an organotin dichloride,[15] we also explored the reactions of **1a,b** with equimolar quantities of Me_2SnCl_2 and Ph_2SnCl_2 in the presence of various proton scavengers. Anion bases (BuLi, KHMDS, LDA), which had been effectively employed in the alkylation of imidazolio-phosphides,[7] reacted in this case non-specifically, presumably because unwanted substitution at Sn–Cl functionalities could not be suppressed. Isolation of any products was unfeasible, and these attempts were abandoned.

Reactions conducted with triethyl amine furnished once more moderate amounts of the intractable precipitates and imidazolium salts [**2a,b**]Cl, but also two new types of soluble products later identified as Lewis adducts **6a,b/7a,b** and imidazolio-distannyl phosphines **8a,b/9a,b**, respectively (Scheme 3). Quite surprising, imidazolio-stannylphosphides arising from simple substitution at the PH-bond in **1a,b** were not detectable. The Lewis adducts **6a,b/7a,b**, which account for approx. 76–78% of the soluble P-containing species (determined by integration of the $^{31}P\{^1H\}$ NMR spectra of crude products), were also identified spectroscopically as the main products of reactions run without the amine, but could not be isolated as separation from other soluble by-products (mainly [**2a,b**]Cl) remained unfeasible. Phosphines **8a,b/9a,b** were only detected in trace amounts when no amine was present. However, they became the dominant products (>80% by ^{31}P NMR analysis of reaction mixtures) when **1a,b** were treated with two equivalents of the organotin dichloride in the presence of excess base and could be isolated in moderate yields (>40%) from these reactions. The product distribution in the reactions studied implies that the assembly of **8a,b** and **9a,b** proceeds in two steps, an initial 1:1 reaction of **1a,b** with a dichlorostannane affording first **6a,b/7a,b**, which may then undergo base-induced dehydrochlorination in the presence of a second equivalent of the electrophile to yield the final products (Scheme 3).

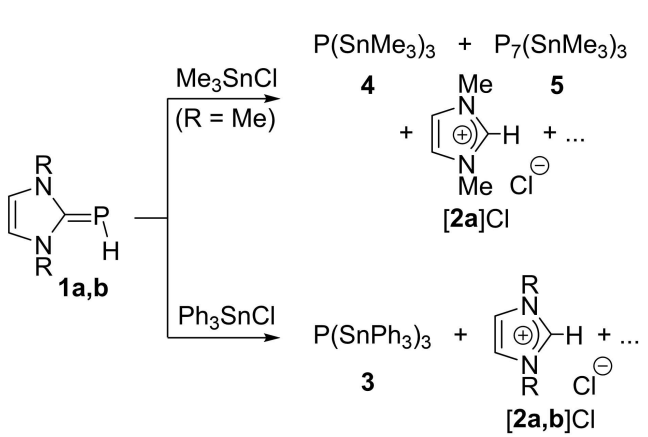

Scheme 2. Reactions of imidazolio-phosphides **1a,b** with Me_3SnCl and Ph_3SnCl (**1a**, **2a**: R = Me; **1b**, **2b**: R = *i*Pr). The same products were obtained when the reactions were carried out in the presence of triethyl amine.

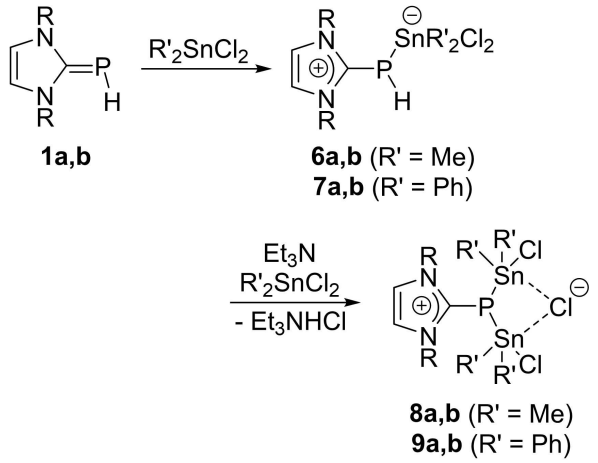

Scheme 3. Reactions of imidazolio-phosphides **1a,b** with Me_2SnCl_2 and Ph_2SnCl_2 and triethyl amine (**1a**, **6a–9a**: R = Me; **1b**, **6b–9b**: R = *i*Pr).

Research Article
doi.org/10.1002/ejic.202101026

The identity of both types of stannylated products was established from spectroscopic data (NMR and IR data for **6a,b**/**7a,b** were derived from the crude products of 1:1 reactions conducted in the absence of the amine). Further confirmation came from single-crystal XRD studies of isolated samples of **8a** and **9a,b** as well as one of a few crystals of **7a** serendipitously grown during prolonged storage of a crude reaction mixture.

Key to the structural assignment of **6a,b** and **7a,b** is the observed splitting of the ^{31}P NMR signals by spin coupling between the phosphorus and directly bonded hydrogen ($^{1}J_{PH}$ = 220–225 Hz) and tin nuclei ($^{1}J_{119SnP}$ = 331–400 Hz). The νPH modes in IR spectra are by some 20–30 cm^{-1} blue-shifted compared to those of **1a,b**, suggesting some strengthening of the PH-bonds upon adduct formation. The single-crystal XRD study on **7a** (Figure 1) confirms the presence of a P–Sn bond (2.534(3) Å) that is shorter than the dative bonds in phosphine complexes of stannanes (typical distances 2.59 ± 0.15) Å[21]) but close to the single bonds in stannyl phosphines (typical distances 2.529 ± 0.042) Å[21]). The tin atom adopts a distorted trigonal bipyramidal coordination (geometry index[22] τ_5 = 0.73) with the chlorine atoms in the apical and the phosphorus atom in one of the equatorial positions. The pyramidal coordination at phosphorus (sum of bond angles 297(6)°) and the presence of a phosphorus-carbon single bond (P1–C13 1.823(4) Å) are common characteristics for imidazolio-phosphide complexes of both main group elements and transition metals.[5,6,12]

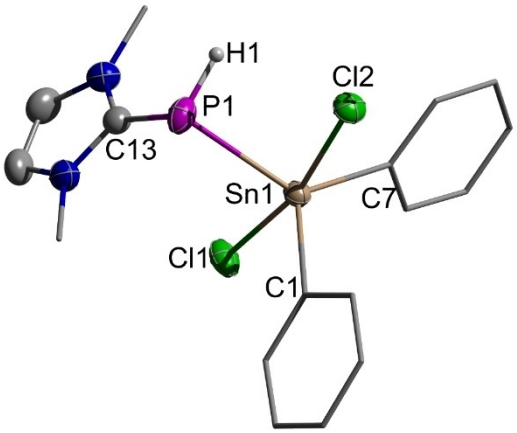

Figure 1. View of the molecular structure of **7a** in the crystal. For clarity, only one position of the disordered PH-moiety is shown, all hydrogen atoms but H1 were omitted, and peripheral substituents were represented using a wire model. Thermal ellipsoids were drawn at the 50% probability level. Selected distances [Å] and angles [°] (values in brackets refer to atoms in the second site of the disordered PH-moiety): P1–C13 1.823(4) [1.837(4)], P1–Sn1 2.534(3) [2.551(3)], P1–H1 1.249(8) [1.250(8)], Sn1–Cl1 2.5173(8), Sn1–Cl2 2.5860(7), C7–Sn1–P1 128.87(11) [C1–Sn1–P1 124.37(12)], Cl1–Sn1–Cl2 168.24(3).

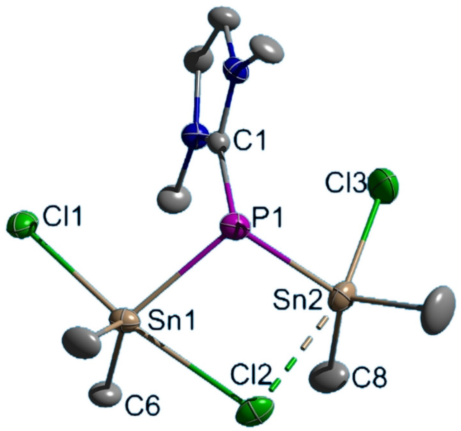

Figure 2. View of the molecular structure of **8a** in the crystal. Hydrogen atoms were omitted for clarity and thermal ellipsoids drawn at the 50% probability level. Selected distances [Å] and angles [°]: Sn1–Cl1 2.4851(9), Sn1–Cl2 2.7917(9), Sn2–Cl2 2.9413(9), Sn2–Cl3 2.4215(10), P1–Sn1 2.5068(8), P1–Sn2 2.5071(9), P1–C1 1.810(3), C6–Sn1–P1 124.35(10), Cl1–Sn1–Cl2 171.72(3), C8–Sn2–P1 126.40(12), Cl2–Sn2–Cl3 165.81(3), Sn1–P1–Sn2 102.10(3), Sn1–Cl2–Sn2 85.67(25).

Crystalline **8a** (Figure 2) and **9a,b** (Figures S1, S2) feature molecular units with a central Sn-P–Sn array made up of a tricoordinate phosphorus and two pentacoordinate tin atoms. The presence of P–Sn and P–C single bonds (P–Sn 2.495(1) to 2.513(1) Å, standard distance 2.529(42) Å;[21] P–C 1.810(3) to 1.818(2) Å, standard distance 1.837(10) Å[23]) and the pyramidal coordination geometry (sum of Sn–P–(Sn,C) angles 316.1(3)° to 321.1(3)°) suggest a local bonding situation around the phosphorus atoms that is archetypal for trivalent phosphines. The tin centers adopt distorted trigonal bipyramidal coordination (with values of 0.55 to 0.79 for the geometry index τ_5) with one μ_2-bridging and two terminal chlorine atoms in the apical positions. The Sn–Cl distances (Sn–μ_1-Cl 2.4215(10) to 2.4880(6) Å, Sn–μ_2-Cl 2.6906(5) to 2.9413(9) Å) compare with those in known chlorostannates (Sn–μ_1-Cl 2.453(89), Sn–μ_2-Cl 2.72(10) Å[21]).

The local environment around the phosphorus and tin atoms and the equivalence of both stannyl units in solution suggest picturing **8** and **9** as cationic phosphines which associate with a chloride anion to form intimate contact ion pairs (Scheme 4, **E**). However, focusing on the asymmetric distortion of the Sn···Cl···Sn unit in the crystalline state (Figure 2), we can also depict these molecules as Lewis adducts between imidazolio-stannylphosphides and organotin dichlorides (Scheme 4, **F**; note that this structure allows one also to rationalize the high chemical fragility of these species, which precluded obtaining meaningful elemental analyses). Keeping in mind that both formulae epitomize merely two different resonance structures of a single species, we do not see a fundamental difference between both representations and

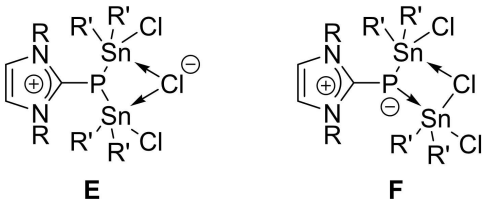

Scheme 4. Two different representations of the bonding in **7** and **8** (R = Me, iPr; R′ = Me, Ph).

Research Article
doi.org/10.1002/ejic.202101026

conclude that the bonding in the cyclic PSn_2Cl array is best described as delocalized.

The constitution of the Lewis pairs **6a**,**b** and **7a**,**b** resembles those of complexes of imidazolio-phosphides with transition metals[5] and the 1:1 adducts with $AlMe_3$ (**10**)[12] or BPh_3 (**11**,[24] Scheme 5), respectively. Similar adducts with dialkyl aluminum and gallium chlorides tBu_2ECl (E = Al, Ga) are also known for dihydroimidazolio-phosphides,[25] but **6** and **7** represent to the best of our knowledge the first cases with a group-14 element as acceptor.

Phosphines **8a**,**b** and **9a**,**b** can be regarded as closely akin to digallium compound **12**[25] and the heterocycles **13**–**17**[25]–[27] (Scheme 5) epitomizing dimers of P-metalated dihydroimidazolio-phosphides. Apart from possessing saturated rather than unsaturated N-heterocycles, group-13 element based **12**–**15** differ from **8** and **9** in comprising shortened P–C bonds (174.4(2) to 175.1(2) Å) and planar coordination at phosphorus. Both features were attributed to a high degree of P–C double bond character,[25,26] which is obviously absent in **8**,**9**. Group-14 based heterocycles **16**, **17**[27] feature still saturated N-heterocycles, but their longer P–C distances (1.796(4) to 1.801(5) Å) and pyramidal coordination of the phosphorus atoms make them in this respect closer structural analogues of **8** and **9**.

The different outcome of the reactions of **1a**,**b** with mono- and dichlorostannanes deserves attention for a number of reasons. To begin with, it appears that the stability of Lewis adducts **6**,**7**, like that of secondary cationic imidazolio-phosphines,[7] does not rely on the steric shielding of the phosphorus reagents. Particularly worth mentioning is that base-induced dehydrohalogenation of **6** and **7** occurs only in the presence of excess Lewis acid and yields imidazolio-distannylphosphines **8**,**9**, whereas cleavage of HCl from the related cationic secondary imidazolio-alkylphosphines requires

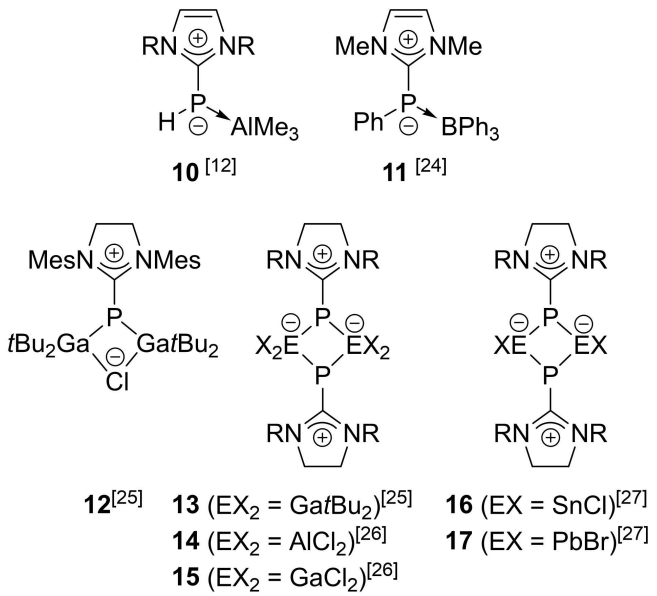

10 [12] **11** [24]

12[25] **13** (EX_2 = Ga*t*Bu$_2$)[25] **14** (EX_2 = $AlCl_2$)[26] **15** (EX_2 = $GaCl_2$)[26] **16** (EX = SnCl)[27] **17** (EX = PbBr)[27]

Scheme 5. Molecular structures of previously reported adducts of (dihydro)imidazolio-phosphides with Lewis acceptors based on group-13 and group-14 elements. (R = Mes, Dipp)

no extra Lewis acid and yields 'simple' imidazolio-alkylphosphides.[7,8] Last, but not least, we note that the reactions of **1a**,**b** with organotin mono- and dichlorides mirror a known dichotomy in the behavior of imidazolio-phenyl-phosphides, which furnish stable Lewis pairs with strong acceptors but react with weakly Lewis acidic triphenylborane under fragmentation to afford NHCs and cyclic oligophosphines $(PPh)_n$.[5,24,28] Analogous dismutation processes occur also during the auto-condensation of secondary imidazolio-phosphines, which are driven by the interaction of the electrophilic phosphorus atom in the phosphine with a nucleophilic imidazolio-phosphide acting as catalyst.[7]

The perceived analogies evoke some important inferences. A generally diverging behavior of imidazolio-phosphides towards weak and strong Lewis acids would also explain the different reactions of **1a**,**b** with tin chlorides. Putting it simply, weak Lewis acids (R'_3SnCl) might furnish equilibrium mixtures of unstable adducts and unreacted imidazolio-phosphides, which could react with each other under PP-bond formation, while sufficiently strong Lewis acids (R'_2SnCl_2) should convert the imidazolio-phosphide into a stable adduct and thus quench the nucleophile needed to initiate a subsequent bond formation step.

Seeking to substantiate these hypotheses, we modelled the behavior of the sterically least protected imidazolio-phosphide **1a** with Me_3SnCl and Me_2SnCl_2 computationally. DFT calculations were carried out at the PCM(THF)-B3LYP-D3BJ/def2-tzvp//PCM(THF)-B3LYP-D3BJ/def2-svp level of theory that had been employed for analyzing the reactivity of primary and secondary imidazolio-phosphines.[7] Assuming that, as in the previous study, the final products form under thermodynamic control, we started with evaluating the energetics of the gross reactions yielding the different types of products observed (Figure 3).

The computed Gibbs free energies indicate that generation of Lewis adduct **18** from **1a** and Me_3SnCl is endoergic (eqn. (1a), $\Delta G^0 = 11.3$ kJ/mol) and thus disfavored compared to exoergic dismutation producing a mixture of **4** and **5** (eqn. (2a), $\Delta G^0 = -12.6$ kJ/mol). In reactions with Me_2SnCl_2, both dismutation to afford **19**/**20** (eqn. (2a), $\Delta G^0 = -26.2$ kJ/mol) and association to yield **6a** (eqn. (1a), $\Delta G^0 = -28.6$ kJ/mol) are exoergic, but Lewis pairing is favored by a slightly higher driving force. Considering reactions with triethylamine, large positive entropy contributions render both base-induced metathesis of **1a** and Me_3SnCl to give stannylated **21** (eqn. (3a), $\Delta G^0 = +34.2$ kJ/mol) and the further assembly of **23** with excess Me_3SnCl (eqn. (4a), $\Delta G^0 = +46.0$ kJ/mol) endoergic, and these reactions are thus out of reach. A different situation emerges for reactions with Me_2SnCl_2, where formation of metathesis product **22** is only slightly endoergic (eqn. (3b), $\Delta G^0 = +3.8$ kJ/mol) and the 2:1 reaction furnishing **8a** strongly exoergic (eqn. (4b), $\Delta G^0 = -52.9$ kJ/mol), making **8a** among all products considered the most stable one.

To analyze the role of the Lewis acid in more detail, we split the gross reactions of eqns. (4a,b) into three steps involving chlorostannane binding to **1a** to yield adducts **6a18**/**6a** according to eqns. (1a,b), dehydrochlorination to form **21**/**22**, and binding of a second chlorostannane to give the final

Research Article
doi.org/10.1002/ejic.202101026

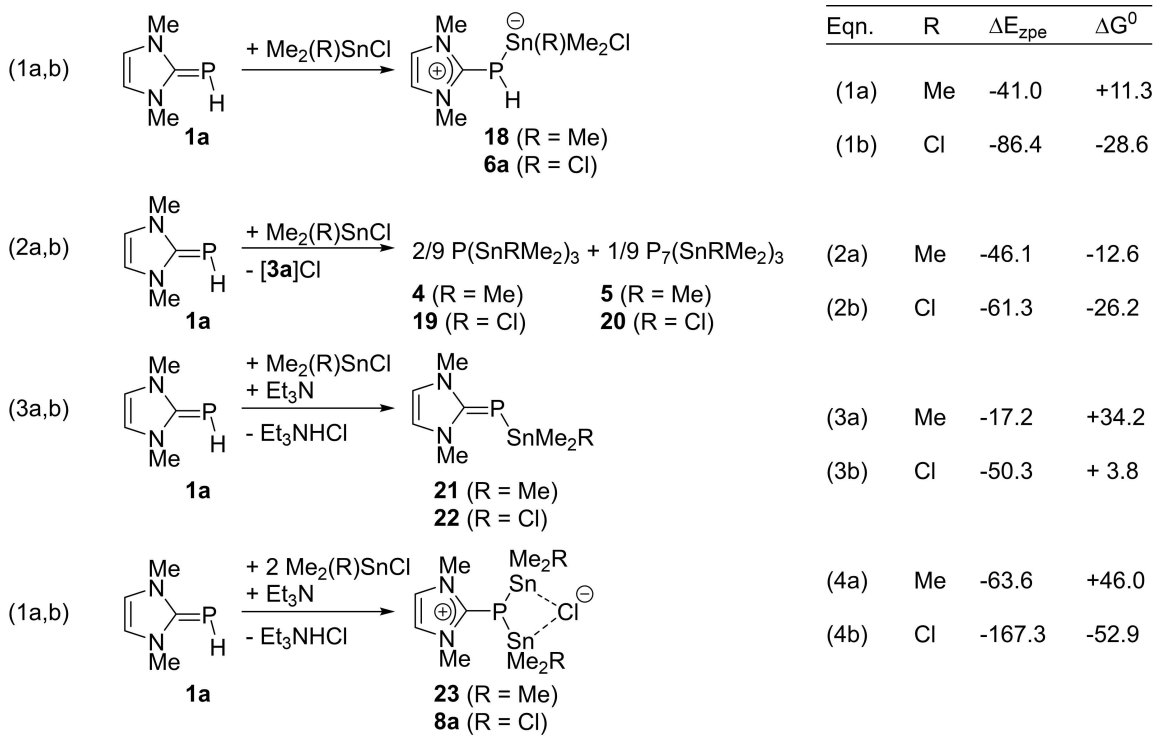

Eqn.	R	ΔE_{zpe}	ΔG^0
(1a)	Me	-41.0	+11.3
(1b)	Cl	-86.4	-28.6
(2a)	Me	-46.1	-12.6
(2b)	Cl	-61.3	-26.2
(3a)	Me	-17.2	+34.2
(3b)	Cl	-50.3	+ 3.8
(4a)	Me	-63.6	+46.0
(4b)	Cl	-167.3	-52.9

Figure 3. Standard free energies ΔG^0 (at 298.13 °C and 1 bar) and electronic energies (including zero-point correction, ΔE_{zpe}) for model reactions represented by equations (1a,b) to (4a,b) computed at the PCM(THF)-B3LYP-3DBJ/def2-tzvp//PCM(THF)-B3LYP-3DBJ/def2-svp level of theory (all values in kJ/mol). R = Me for eqns. (1a) to (4a) and R = Cl for eqns. (1b) to (4b).

products **23**/**8a** (Figure 4; see that although all reactions are represented as unidirectional for clarity, they must in fact be considered reversible).[29] Note that both Lewis pair formation steps are entropically unfavorable and we expect exoergic transformations only when sufficiently large negative energy terms offset the entropy effects.

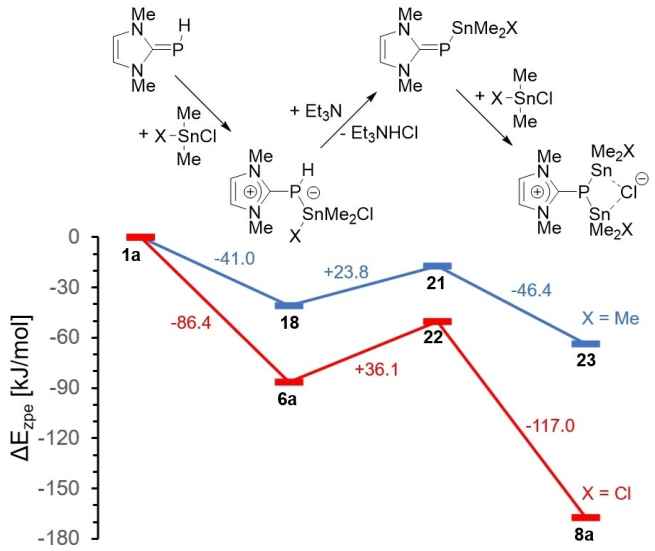

Figure 4. Delineation of the formation of **8a**/**23** according to eqns. (4a,b) into elementary steps and associated energy profile. Values of ΔE_{zpe} were computed from electronic energies obtained at the PCM(THF)-B3LYP-3DBJ/def2-tzvp//PCM(THF)-B3LYP-3DBJ/def2-tzvp level and zero-point corrections derived from frequency calculations with the smaller basis set and are given in kJ/mol.

The calculated energy profiles reveal that Lewis pairing is indeed generally exothermic and the dehydrochlorination is endothermic. Moreover, formal exchange of Me_3SnCl by more Lewis acidic Me_2SnCl_2 renders adduct formation with both **1a** and the corresponding imidazolio-stannylphosphide (**22**) energetically more favorable (by 45.4 and 70.6 kJ/mol), but disfavors HCl abstraction (by 12.3 kJ/mol). This inhibiting effect is at first glance surprising in view of the proton affinities for the conjugate bases of **21** (1463 kJ/mol) and **22** (1415 kJ/mol), which suggest an increase in PH-acidity with higher electron withdrawing power of the Lewis acid, but can be explained by recalling that **6a** is also more reluctant than **18** to release a chloride. On the whole, it appears that the driving force derived from binding of two weakly Lewis acidic molecules of Me_3SnCl or a single molecule of Me_2SnCl_2 is too small to compensate for the unfavorable entropy change and the endothermic dehydrohalogenation steps associated with creation of **21**–**23**. In contrast, the excess energy released upon binding of a second equivalent of the stronger electrophile Me_2SnCl_2 suffices as a booster that can turn the overall reaction according to eqn. (4b) into an exoergic process and shifts the equilibrium to the product side.

Having confirmed that the route to dismutation products **3**,**5** is thermodynamically feasible, we wanted to establish if it is also kinetically viable. Presuming that PP-bond formation

Research Article
doi.org/10.1002/ejic.202101026

during creation of **5** is achieved, as previously proposed,[7] by interaction of nucleophilic imidazolio-phosphides with suitable electrophiles, we focused on analyzing the reaction of **1a** with **18** as a model case. Our studies suggest indeed that the imidazolio-phosphide may react with neutral **18** in the same way as with a cationic imidazolio-phosphine to produce first diphosphine **24** and a transient carbene, which can then exchange a proton to yield zwitterionic diphosphide **25** and imidazolium ion $[\mathbf{2a}]^+$ (Figure 5). A relaxed potential energy scan (Figure S44) indicates that, like in reactions with imidazolio-phosphines,[7] PP-bond formation does not require passing an energy barrier. Lewis pairing of **25** with Me_3SnCl may further furnish **26**, which can possibly act as electrophile in further PP-bond formation steps.

In contrast to condensations with cationic imidazolio-phosphines,[7] the reactions leading to **25** and **26** are endoergic, and we cannot expect the coupling products to be observable intermediates. However, with follow-up processes yielding larger PP-bonded frameworks becoming increasingly more favorable,[7] diphosphine formation may still be considered the first step in a reaction cascade of mutually coupled equilibria enabling the assembly of **5** or other polyphosphorus species as final products. The origin of **4** as by-product was not evaluated in detail, but is likely to result from dismutation processes that are quite common in the chemistry of polyphosphines[30] and had also been observed in the condensation of imidazolio-phosphines.[7] The kinetic viability of condensation reactions could also explain the low stability and unselective formation of **6a** if we assume that any encounter of **6a** with unreacted **1a** during the course of the reaction is likely to induce a practically irreversible formation of polyphosphorus species and imidazolium salts.

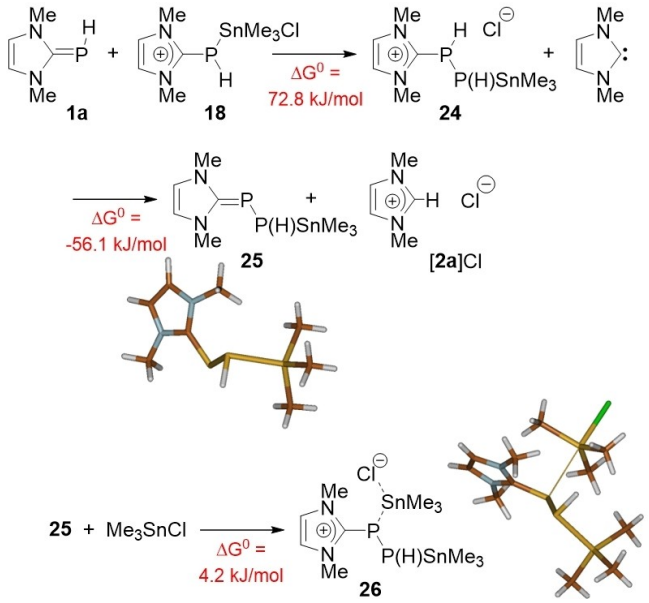

Figure 5. Proposed two-step condensation of **1a** and **18** to afford **25** and further reaction with Me_3SnCl to form **26**. Gibbs free energies were computed as outlined in Figure 4. The computed molecular structures of **25** and **26** are shown in wireframe representation.

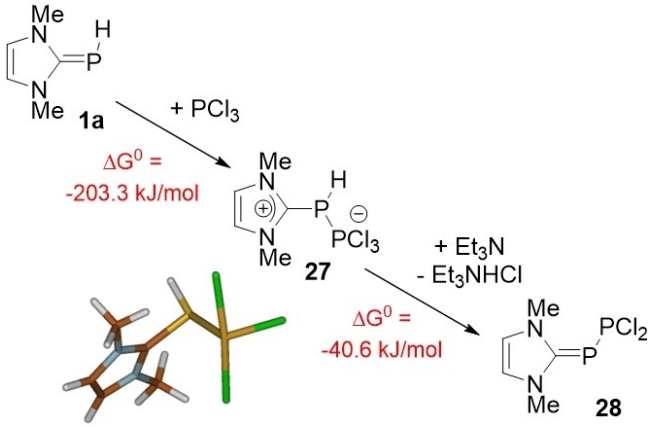

Figure 6. Calculated Gibbs free energies (at the PCM(THF)-B3LYP-3DBJ/def2-tzvp//PCM(THF)-B3LYP-3DBJ/def2-tzvp level) for the reaction of **1a** with PCl_3 and Et_3N. The molecular structure of **27** is shown in wireframe representation.

Noting that imidazolio-stannylphosphides **21/22** were in none of the reactions studied in this work the preferred products, whereas successful base-induced PH-substitution in primary imidazolio-phosphides with chlorophosphines (including PCl_3) is known,[3,9] we wondered if our computational model suffices to reproduce and possibly even explain this divergence as well. Modelling accordingly also the hypothetic reaction of **1a** with PCl_3 (Figure 6), we found that initial formation of Lewis pair **27** showing a similar see-saw configuration as adducts of phosphorus trihalides with N-heterocyclic carbenes[31] is even more favorable than assembly of **6a**, and that HCl abstraction with triethylamine to yield **28** is now exoergic. A higher binding energy for PCl_3 ($\Delta E_{zpe} = -274.9$ kJ/mol) than for Me_2SnCl_2 and a relatively low proton affinity of the conjugate base of **27** (1381 kJ/mol) attest that PCl_3 acts both as a stronger Lewis acid and exerts a larger acidifying effect on the PH-bond of **1a**.

Conclusion

Reactions of imidazolio-phosphides with organotin chlorides and tertiary amines (Et_3N, DABCO, DBU) do not proceed under substitution at the PH-bond. Diorganotin dichlorides initially produce a Lewis adduct, which then reacts with the base and excess electrophile to afford chlorido-complexes of cationic imidazolio-distannylphosphines. Reactions with triorganotin chlorides proceed under dismutation to afford stannylated (oligo)phosphines and phosphorus-free imidazolium salts beside some intractable solids. Computational studies suggest relating the deviating reaction patterns with competing reaction channels whose key steps resemble those encountered in reactions of imidazolio-phosphides with acids.[7] Case studies indicate that the product selectivity depends decisively on the electrophilic character of the Lewis acid involved and allowed identifying three different scenarios. Action of weak electrophiles (e.g. R_3SnCl) produces unstable Lewis-adducts that exist only in equilibrium with unreacted imidazolio-phosphides and

Research Article
doi.org/10.1002/ejic.202101026

may interact with these under PP-bond formation and eventual assembly of polyphosphorus species. Medium strong electrophiles (e.g. R_2SnCl_2) completely consume the imidazolio-phosphide to form stable Lewis-adducts, which may undergo endoergic deprotonation if the resulting product is stabilized by binding of a further Lewis acid. Finally, still stronger electrophiles (e.g. PCl_3) give rise to Lewis pairs that are sufficiently PH-acidic to transfer a proton to an auxiliary base in an exoergic step. The proposed categorization offers a rationale for previous reports on diverging reactivity patterns of imidazolio-phosphides towards other electrophiles than chlorostannanes,[28] and permits to infer valuable guidelines for the design of further synthetic applications for these molecules.

Experimental Section

All manipulations were carried out under an atmosphere of inert argon inside glove boxes or by using standard vacuum line techniques. Solvents were dried by literature known procedures. NMR spectra were recorded on Bruker Avance 250 (^{1}H 250.0 MHz, ^{13}C 62.9 MHz, ^{31}P 101.2 MHz, ^{119}Sn 93.2 MHz) or Avance 400 (^{1}H 400.1 MHz, ^{13}C 100.5 MHz, ^{31}P 161.9 MHz, ^{119}Sn 149.2 MHz) instruments at 293 K if not stated otherwise. ^{1}H Chemical shifts were referenced to TMS using the signals of the residual protons of the deuterated solvent (δ^1H = 7.24 ($CDCl_3$), 7.15 (C_6D_6), 1.96 (CD_3CN), 1.73 (THF-D_8)) as secondary reference. Spectra of heteronuclei were referenced using the Ξ-scale employing TMS (Ξ = 25.145020 MHz, ^{13}C), 85 % H_3PO_4 (Ξ = 40.480747 MHz, ^{31}P) and $SnMe_4$ (Ξ = 37.290655 MHz, ^{119}Sn) as secondary references. The ^{13}C{^{1}H} NMR signals of quaternary carbon atoms were mostly unidentifiable due to insufficient signal-to-noise ratio and signal broadening effects. ^{119}Sn NMR spectra were recorded using the DEPT pulse sequence. Coupling constants involving tin nuclei refer to the isotope ^{119}Sn if not stated otherwise. Analysis of NMR spectra by iterative simulation was carried out using the DAISY module implemented in the Bruker Topspin software with $^1J_{PP}$ couplings being assumed as negative. The FTIR spectra were recorded with a Thermo Scientific/Nicolet iS5 instrument equipped with an iD5 attenuated total reflectance (ATR) accessory. Elemental analyses were determined on a Thermo Micro Cube CHN analyzer. Imidazolio-phosphides were prepared as reported elsewhere.[7]

Reaction of 1a with Me_3SnCl: (a) **1a** (100 mg, 780 μmol) and Me_3SnCl (156 mg, 780 μmol) were dissolved in THF or MeCN (20 mL). The mixture was stirred for 24 h to produce an orange-colored solution and a dark red precipitate. Volatiles were evaporated. The residue was extracted with pentane (20 mL), insoluble solids removed by filtration, and the filtrate evaporated. NMR spectroscopic analysis of the residual semi-solid (see Figure S4) disclosed the presence of $P(SnMe_3)_3$ (**4**).

(b) The reaction was carried out as before and the residue left behind after evaporation of the reaction mixture extracted with C_6D_6. The extract was analyzed by ^{31}P{^{1}H} NMR spectroscopy (Figure S5). Spectral simulation of the observed line pattern disclosed the presence of $P(SnMe_3)_3$ (**4**) and $P_7(SnMe_3)_3$ (**5**). The data obtained from the simulation are consistent with literature data.[19,20]

$P(SnMe_3)_3$ (**4**): ^{1}H NMR (C_6D_6): δ = 0.30 (d, $^3J_{P,H}$ = 3 Hz, $^3J_{Sn,H}$ = 54 Hz, 27 H, $SnCH_3$). – ^{13}C{^{1}H} NMR (C_6D_6): δ = −3.8 (d, $^2J_{PC}$ = 6 Hz, $SnCH_3$). – ^{31}P{^{1}H} NMR (C_6D_6): δ = −328.1 (s, $^1J_{SnP}$ = 798 Hz). – ^{119}Sn{^{1}H} NMR (C_6D_6): δ = 39.2 (d, $^1J_{SnP}$ = 798 Hz).

$P_7(SnMe_3)_3$ (**5**): ^{31}P{^{1}H} NMR (C_6D_6): δ = −13.8 (m), −83.4 (m), −159.1 (m), simulated as A[MX]$_3$ spin system with parameters: δ^A −83.4, δ^M −13.8, δ^X −159.1, $^1J_{AM}$ = −304 Hz, $^2J_{AX}$ = 55 Hz, $^2J_{MM'}$ = −11 Hz, $^1J_{MX}$ = −343 Hz, $^2J_{MX'}$ = 10 Hz, $^1J_{XX'}$ = −215 Hz.

Reactions of imidazolio-phosphides 1a,b with Ph_3SnCl: Imidazolio-phosphide (100 mg, **1a**: 780 μmol/**1b**: 543 μmol) and Ph_3SnCl (301 mg/780 μmol or 209 mg/543 μmol, respectively) were dissolved in THF or MeCN (20 mL). The mixture was stirred for 24 h to produce an orange-colored solution and a dark precipitate. Volatiles were evaporated, the residue extracted with pentane (20 mL), and the resulting extract once more evaporated to dryness. Characterization of the remaining colorless solid (from **1b**) or semi-solid (from **1a**) by NMR spectroscopy (Figures S6, S7) disclosed the presence of $P(SnPh_3)_3$ (**3**, from **1b**) or a 36:64 mixture of **3** and $PH(SnPh_3)_2$ (from **1a**) as the only phosphorus-containing species. The NMR data is consistent with reported values.[17]

$P(SnPh_3)_3$ (**3**): ^{31}P{^{1}H} NMR (THF): δ = −327.3 (s, $^1J_{SnP}$ = 877 Hz). – ^{119}Sn{^{1}H} NMR (THF): δ = −68.5 (d, $^1J_{SnP}$ = 876 Hz, $^2J_{119Sn117Sn}$ = 279 Hz).

$PH(SnPh_3)_2$: ^{31}P NMR (toluene): δ = −315.2 (d, $^1J_{PH}$ = 166.6 Hz).

Imidazolio-bis(diorganochlorostannyl)-phosphine chlorides 8, 9. (a) 1:1 Reactions: Stoichiometric amounts of imidazolio-phosphides (100 mg, **1a**: 780 μmol, **1b**: 543 μmol) and organotin dichlorides (Me_2SnCl_2: 780 μmol, Ph_2SnCl_2: 543 μmol) were dissolved in THF (20 mL). Excess triethylamine (7.81/5.41 mmol) was added. The yellow solutions were stirred for 1 h at rt and filtered over Celite. The filtrates were evaporated to dryness, the residues washed with n-pentane, and dried in vacuum. The crude products were dissolved in $CDCl_3$. Analysis by ^{31}P NMR spectroscopy revealed the presence of mixtures containing **8a,b**/**9a,b** and **6a,b**/**7a,b** as phosphorus-containing components (relative concentrations determined by spectral integration: **8a**:**6a** 24:76 from **1a**/$SnMe_2Cl_2$; **8b**:**6b** 23:77 from **1b**/$SnMe_2Cl_2$; **9a**:**7a** 22:78 from **1a**/$SnPh_2Cl_2$; **9b**:**7b** 24:76 from **1b**/$SnPh_2Cl_2$).

(b) 1:2 Reactions: Imidazolio-phosphide (100 mg, **1a**: 780 μmol, **1b**: 543 μmol) and the appropriate organotin dichloride (1.56 mmol/1.08 mmol) were dissolved in THF (20 mL). A tenfold excess of triethyl amine (7.81 mmol/5.40 mmol) was added. The resulting yellow solutions were stirred for 1 h at rt. The volume of the solution was then reduced to one third under reduced pressure and the residual mixture filtered over Celite. The filtrates were evaporated to dryness. The products **8a**,**b** and **9a**,**b** were isolated by washing the remaining yellow solids with n-pentane (2 mL) and drying in vacuum.

8a: Yield 219 mg (410 μmol, 53 %). – ^{1}H NMR (THF-D_8): δ = 7.48 (s, 2 H, =CH), 4.01 (s, 6 H, NCH_3), 1.04 (s, 12 H, $^3J_{SnH}$ = 69 Hz, $SnCH_3$). – ^{13}C{^{1}H} NMR (THF-D_8): δ = 123.8 (s, =CH), 37.4 (s, NCH_3), 8.9 (s, $SnCH_3$). – ^{31}P NMR (THF-D_8): δ = −162.0 (s, $^1J_{SnP}$ = 533 Hz). – ^{119}Sn{^{1}H} NMR (THF-D_8): δ = −67.0 (d, $^1J_{SnP}$ = 533 Hz).

8b: recrystallization from 1,2-dichloroethane furnished a small yield of product containing 0.75 molecules of C_2H_4Cl per formula unit (by ^{1}H NMR); no yield determined. ^{1}H NMR ($CDCl_3$): δ = 7.28 (s, 2 H, =CH), 5.34 (dsept, $^3J_{HH}$ = 6.6 Hz, $^4J_{PH}$ = 4,7 Hz, 2 H, NCH), 1.62 (d, 12 H, $^3J_{HH}$ = 6.7 Hz, CH_3), 1.16 (d, 12 H, $^3J_{SnH}$ = 68.4 Hz, $^3J_{PH}$ = 1.7 Hz, $SnCH_3$). – ^{13}C{^{1}H} NMR ($CDCl_3$): δ = 147.7 (d, $^1J_{PC}$ = 85.7 Hz, CP), 119.6 (s, =CH), 52.7 (d, $^3J_{PC}$ = 9.2 Hz, NCH), 22.6 (s, CH_3), 9.7 (s, $^2J_{PC}$ = 7.1 Hz, $SnCH_3$). – ^{31}P NMR ($CDCl_3$): δ = −156.6 (s, $^1J_{SnP}$ = 577 Hz). – ^{119}Sn{^{1}H} NMR ($CDCl_3$): δ = −60.8 (d, $^1J_{SnP}$ = 578 Hz, $^2J_{119Sn117Sn}$ = 184 Hz).

9a: Rapid crystallization from THF/pentane furnished a yield of 351 mg of an impure product which sufficed to obtain NMR data and pick a single-crystal suitable for XRD. The occurrence of unspecific decay processes during recrystallization precluded obtaining analytically pure samples. ^{1}H NMR (THF-D_8): δ = 8.03 (m,

$^3J_{SnH}$ = 81 Hz, 8 H, Ph), 7.51 (s, 2 H, =CH), 7.31–7.25 (m, 12 H, Ph), 3.84 (s, 6 H, NCH_3). – $^{13}C\{^1H\}$ NMR (THF-D_8): δ = 136.0 (s, Ph). 129.0 (s, Ph), 127.9 (s, Ph), 124.1 (s, =CH), 37.7 (s, NCH_3). – ^{31}P NMR (THF-D_8): δ = −149.2 (s, $^1J_{SnP}$ = 523 Hz). – $^{119}Sn\{^1H\}$ NMR (THF-D_8): δ = −188.9 (d, $^1J_{SnP}$ = 523 Hz).

9 b: Yield 195 mg (0.23 mmol, 43 %). – ^1H NMR (THF-D_8): δ = 8.10 (m, $^3J_{SnH}$ = 82 Hz, 8 H, *o*-Ph), 7.72 (s, 2 H, =CH), 7.34–7.27 (m, 12 H, *m/p*-Ph), 5.28 (m, 2 H, NCH), 1.27 (d, $^3J_{HH}$ = 6.2 Hz, 12 H, CH_3). – $^{13}C\{^1H\}$ NMR (THF-D_8): δ = 136.1 (s, *o*-Ph), 129.0 (s, *m*-Ph), 127.9 (s, *p*-Ph), 120.6 (s, =CH), 52.7 (s, NCH), 22.2 (s, CH_3). – ^{31}P NMR (THF-D_8): δ = −144.3 (s, $^1J_{SnP}$ = 528 Hz). – $^{119}Sn\{^1H\}$ NMR (THF-D_8): δ = −195.8 (d, $^1J_{SnP}$ = 526 Hz). – $C_{33}H_{37}Cl_3N_2PSn_2$ (836.42 g mol^{-1}): calcd. C 47.39 H 4.46 N 4.45, found C 46.77 H 4.22 N 3.76.

Spectroscopic identification of Lewis adducts 6, 7. Stoichiometric amounts of **1 a** (100 mg, 0.780 mmol) or **1 b** (100 mg, 0.543 mmol) and the appropriate organotin dichlorides (Me_2SnCl_2: 0.780 mmol; Ph_2SnCl_2: 0.543 mmol) were dissolved in THF (20 mL). The resulting yellow solutions were stirred for 1 min and filtered over Celite. The filtrates were evaporated to dryness. The remaining yellow solids were washed with pentane, dried under vacuum, and dissolved in $CDCl_3$. Characterization by NMR spectroscopy (see Figures S34 to S39) revealed the presence of mixtures containing **6 a,b/7 a,b** as main products (up to 80 %) besides imidazolium salts [**2 a,b**]Cl (NMR data match reported ones and are not repeated here) and traces of **8 a,b/9 a,b**.

6 a: ^1H NMR ($CDCl_3$): δ = 7.18 (s, 2 H, =CH), 3.94 (d, $^1J_{PH}$ = 220 Hz, $^2J_{SnH}$ = 50 Hz, 1 H, PH), 3.91 (s, 6 H, NCH_3), 1.18 (br, 6 H, $SnCH_3$). – $^{13}C\{^1H\}$ NMR ($CDCl_3$): δ = 123.6 (br, =CH), 37.6 (d, $^3J_{PC}$ = 5 Hz, NCH_3), 12.5 (br, $SnCH_3$). – ^{31}P NMR ($CDCl_3$): δ = −166.0 (d, $^1J_{PH}$ = 220 Hz, $^1J_{SnP}$ = 394 Hz. – $^{119}Sn\{^1H\}$ NMR ($CDCl_3$): δ = −116.4 (d, $^1J_{SnP}$ = 394 Hz). – IR (crude prod.): ν (cm^{-1}) = 2330 (w) (νPH).

6 b: ^1H NMR ($CDCl_3$): δ = 7.23 (s, 2 H, =CH), 4.93 (m, 2 H, CH), 3.96 (d, $^1J_{PH}$ = 215 Hz, $^2J_{SnH}$ = 54 Hz, 1 H, PH), 1.53 (br, 12 H, CH_3), 1.16 (br s, 6 H, $SnCH_3$). – $^{13}C\{^1H\}$ NMR ($CDCl_3$): δ = 119.0 (d, $^3J_{PC}$ = 1.3 Hz, =CH), 52.3 (d, $^3J_{PC}$ = 7.1 Hz, CH), 23.1 (s, CH_3), 22.6 (s, CH_3), 11.7 (br, $SnCH_3$). – ^{31}P NMR ($CDCl_3$): δ = −168.5 (d, $^1J_{PH}$ = 221 Hz, $^1J_{SnP}$ = 400 Hz). – $^{119}Sn\{^1H\}$ NMR ($CDCl_3$): δ = −124.0 (d, $^1J_{SnP}$ = 400 Hz). – IR (crude prod.): ν (cm^{-1}) = 2350 (m) (νPH).

7 a: ^1H NMR ($CDCl_3$): δ = 8.21 (m, $^3J_{SnH}$ = 88 Hz, 4 H, Ph), 7.40–7.31 (m, 6 H, Ph), 7.04 (s, 2 H, =CH), 4.16 (d, $^1J_{PH}$ = 221 Hz, $^2J_{SnH}$ = 60 Hz, 1 H, PH), 3.71 (d, $^3J_{PH}$ = 3.7 Hz, 6 H, CH_3). – $^{13}C\{^1H\}$ NMR ($CDCl_3$): δ = 145.1 (s, *i*-Ph), 136.3 (s, *o*-Ph), 129.3 (s, *p*-Ph), 128.3 (s, *m*-Ph), 123.4 (br s, =CH), 37.6 (br d, $^2J_{PC}$ = 5 Hz, CH_3). – ^{31}P NMR ($CDCl_3$): δ = −163.2 (d, $^1J_{PH}$ = 221 Hz, $^1J_{SnP}$ = 331 Hz). – $^{119}Sn\{^1H\}$ NMR ($CDCl_3$): δ = −242.1 (d, $^1J_{SnP}$ = 331 Hz). – IR (crude prod.): ν (cm^{-1}) = 2341 (m) (νPH).

7 b: ^1H NMR ($CDCl_3$): δ = 8.16 (m, $^3J_{SnH}$ = 83 Hz, 4 H, Ph), 7.4–7.2 (m, 6 H, Ph), 7.05 (s, $^5J_{SnH}$ = 5 Hz, 2 H, =CH), 4.74 (dsept, $^3J_{HH}$ = 6.8 Hz, $^4J_{PH}$ = 2.5 Hz, 2 H, CH) 4.09 (d, $^1J_{PH}$ = 224 Hz, $^2J_{SnH}$ = 60 Hz, 1 H, PH), 1.32 (d, $^3J_{HH}$ = 6.8 Hz, 6 H, CH_3), 1.13 (d, $^3J_{HH}$ = 6.8 Hz, 6 H, CH_3). – $^{13}C\{^1H\}$ NMR ($CDCl_3$): δ = 148.2 (d, $^1J_{PC}$ = 67 Hz, PC), 144.9 (d, $^2J_{PC}$ = 3.6 Hz, SnC), 136.5 (s, $^3J_{SnC}$ = 62 Hz, *m*-Ph), 129.2 (s, $^4J_{SnC}$ = 18 Hz, *p*-Ph), 128.2 (s, $^2J_{SnC}$ = 83 Hz, *o*-Ph), 119.2 (d, $^3J_{PC}$ = 2 Hz, =CH), 52.5 (d, $^3J_{PC}$ = 7 Hz, CH), 22.9 (s, CH_3), 22.2 (s, CH_3). – ^{31}P NMR ($CDCl_3$): δ = −165.7 (d, $^1J_{PH}$ = 224 Hz, $^1J_{SnP}$ = 342 Hz). – $^{119}Sn\{^1H\}$ NMR ($CDCl_3$): δ = −244.8 (d, $^1J_{SnP}$ = 342 Hz). – IR (crude prod.): ν (cm^{-1}) = 2368 (m) (νPH).

Crystallographic Studies. Single-crystal X-ray diffraction data were measured on a Bruker Kappa APEX2 Duo diffractometer at 130(2) K for **9 b**, 135(2) K for **9 a** and **7 a**, and 140(2) K for **8 a**, respectively, using Mo K_α radiation (λ = 0.71073 Å) for **8 a**, **9 a,b**, and Cu Kα-radiation (λ = 1.54178 Å) for **7 a**. The structures were solved by direct methods (SHELXS-2014[32]) and refined with a full-matrix-least-squares scheme on F^2 (SHELXL-2014[32]). Semi-empirical absorption corrections from equivalents were applied for **7 a** and **8 a**, and numerical absorption corrections for **9 a,b**. Non-hydrogen atoms were refined anisotropically. The PH-moiety of **7 a** was disordered over two positions and was refined using restraints with the occupancy being determined from free refinement at the isotropic stage and being fixed at 55:45 during the anisotropic refinement. Potential disorders of one phenyl moiety and the hydrogen atoms in one methyl group were not resolved. A general RIGU restraint was used in the refinement. Further crystallographic data and details on the structure solution are given in the Supporting Information.

Computational Studies. DFT calculations were carried out with the Gaussian 16 program package.[33] Full geometry optimization was performed at the PCM(THF)-B3LYP-3DBJ/def2-svp level, using the B3LYP functional[34] with Grimme's dispersion corrections with Becke-Johnson damping,[35] basis sets from Ahlrichs' and Weigend's def2-family,[36] and the polarizable continuum model (PCM) implemented in the Gaussian program to simulate solvent effects. Harmonic vibrational frequency calculations were carried out at the same level to establish the nature of the stationary points obtained as local minima or transition states. Standard Gibbs free energies ΔG^0 and electronic energies E_{zpe} including zero-point corrections were computed by combining electronic energies recalculated at the PCM(THF)-B3LYP-3DBJ/def2-tzvp level with the corrections obtained from the frequency calculations with the smaller basis set. Proton affinities were calculated as the negative of the enthalpy change associated with the reaction of the species under consideration with a proton in the gas phase, using B3LYP-3DBJ/def2-tzvp energies with the corrections obtained from the frequency calculations with the smaller basis set. MOLDEN[37] was used for visualization.

Deposition Numbers 2083820 (for **9 b**), 2083821 (for **9 a**), 2083822 (for **7 a**), and 2083824 (for **8 a**) contain the supplementary crystallographic data for this paper. These data are provided free of charge by the joint Cambridge Crystallographic Data Centre and Fachinformationszentrum Karlsruhe Access Structures service www.ccdc.cam.ac.uk/structures.

Acknowledgements

The authors gratefully acknowledge financial support from German Research Foundation (DFG) grant no Gu415-17/1 and thank B. Förtsch for elemental analyses and Dr. W. Frey (Institut für Organische Chemie) for collecting the x-ray data sets. The computational studies were supported by the state of Baden-Württemberg through bwHPC and the German Research Foundation (DFG) through grant no INST 40/467-1 FUGG (JUSTUS cluster). Open Access funding enabled and organized by Projekt DEAL.

Conflict of Interest

The authors declare no conflict of interest.

Data Availability Statement

The data that support the findings of this study are available in the supplementary material of this article.

Keywords: Donor-acceptor systems · Phosphides · Reaction mechanisms · Substituent effects · Tin

[1] K. Hansen, T. Szilvási, B. Blom, S. Inoue, J. Epping, M. Driess, *J. Am. Chem. Soc.* **2013**, *135*, 11795–11798.
[2] A. Doddi, D. Bockfeld, T. Bannenberg, P. G. Jones, M. Tamm, *Angew. Chem. Int. Ed.* **2014**, *53*, 13568–13572; *Angew. Chem.* **2014**, *126*, 13786–13790.
[3] A. M. Tondreau, Z. Benkő, J. R. Harmer, H. Grützmacher, *Chem. Sci.* **2014**, *5*, 1545–1554.
[4] M. Cicač-Hudi, J. Bender, S. H. Schlindwein, M. Bispinghoff, M. Nieger, H. Grützmacher, D. Gudat, *Eur. J. Inorg. Chem.* **2016**, 649–658.
[5] For recent reviews on the chemistry of **A**, see: a) T. Krachko, J. C. Slootweg, *Eur. J. Inorg. Chem.* **2018**, 2734–2754; b) A. Doddi, M. Peters, M. Tamm, *Chem. Rev.* **2019**, *119*, 6994–7112.
[6] L. Liu, D. A. Ruiz, F. Dahcheh, G. Bertrand, *Chem. Commun.* **2015**, *51*, 12732–12735.
[7] M. Cicač-Hudi, C. M. Feil, N. Birchall, M. Nieger, D. Gudat, *Dalton Trans.* **2020**, *49*, 17401–17413.
[8] J. E. Rodriguez Villanueva, M. A. Wiebe, G. G. Lavoie, *Organometallics* **2020**, *39*, 3260–3267.
[9] A. Beil, R. J. Gilliard, H. Grützmacher, *Dalton Trans.* **2016**, *45*, 2044–2052.
[10] Z. Kelemen, R. Streubel, L. Nyulászi, *RSC Adv.* **2015**, *5*, 41795–41802.
[11] L. Weber, *Eur. J. Inorg. Chem.* **2000**, 2425–2441.
[12] J. Bhattacharjee, M. Peters, D. Bockfeld, M. Tamm, *Chem. Eur. J.* **2021**, *27*, 5913–5918.
[13] M. Bispinghoff, A. M. Tondreau, H. Grützmacher, C. A. Faradji, P. G. Pringle, *Dalton Trans.* **2016**, *45*, 5999–6003.
[14] Z. Li, X. Chen, Y. Li, C.-Y. Su, H. Grützmacher, *Chem. Commun.* **2016**, *52*, 11343–11346.
[15] M. Balmer, C. v. Hänisch, *Z. Anorg. Allg. Chem.* **2018**, *644*, 1143–1148.
[16] Y. Wang, Y. Xie, M. Y. Abraham, R. J. Gilliard, P. Wei, H. F. Schaefer, P. v. R. Schleyer, G. H. Robinson, *Organometallics* **2010**, *29*, 4778–4780.
[17] C. C. Cummins, C. Huang, T. J. Miller, M. W. Reintinger, J. M. Stauber, I. Tannou, D. Tofan, A. Toubaei, A. Velian, G. Wu, *Inorg. Chem.* **2014**, *53*, 3678–3687.
[18] Reaction of **1a** with Ph_3SnCl afforded a 36:64 mixture of $P(SnPh_3)_3$ and a product assigned as $PH(SnPh_3)_2$ (see Experimental Section).
[19] H. Schumann, P. Schwabe, O. Stelzer, *Chem. Ber.* **1969**, *102*, 2900–2913.
[20] G. Fritz, K. D. Hoppe, W. Hönle, D. Weber, C. Mujica, V. Manriquez, H. G. v. Schnering, *J. Organomet. Chem.* **1983**, *249*, 63–80.
[21] The values represent the median and standard deviation of the distances returned by appropriate queries in the CSD database (CSD 5.41 updated May 2020).
[22] A. W. Addison, N. T. Rao, J. Reedijk, J. van Rijn, G. C. Verschoor, *J. Chem. Soc. Dalton Trans.* **1984**, 1349–1356.
[23] F. H. Allen, O. Kennard, D. G. Watson, L. Brammer, G. A. Orpen, R. A. Taylor, *J. Chem. Soc. Perkin Trans. 2* **1987**, S1–S19.
[24] T. Krachko, M. Bispinghoff, A. M. Tondreau, D. Stein, M. Baker, A. W. Ehlers, J. C. Slootweg, H. Grützmacher, *Angew. Chem. Int. Ed.* **2017**, *56*, 7948–7951; *Angew. Chem.* **2017**, *129*, 8056–8059.
[25] O. Lemp, M. Balmer, K. Reiter, F. Weigend, C. von Hänisch, *Chem. Commun.* **2017**, *53*, 7620–7623.
[26] M. Balmer, C. von Hänisch, *Z. Anorg. Allg. Chem.* **2020**, *646*, 648–652.
[27] M. Balmer, Y. J. Franzke, F. Weigend, C. von Hänisch, *Chem. Eur. J.* **2020**, *26*, 192–197.
[28] A. J. Arduengo, C. J. Carmalt, J. A. C. Clyburne, A. H. Cowley, R. Pyati, *Chem. Commun.* **1997**, 981–982.
[29] An alternative scheme assuming binding of the second Lewis acid prior to deprotonation is likewise conceivable given the ability of imidazoliophosphides to bind two Lewis acids, but was disregarded as the molecular structures of the 2:1 adducts lack a second dative SnP-bond and resemble rather van-der-Waals complexes of chlorostannanes.
[30] a) M. Baudler, K. Glinka, *Chem. Rev.* **1993**, *93*, 1623–1667; b) M. Baudler, K. Glinka, *Chem. Rev.* **1994**, *94*, 1273–1297.
[31] a) Y. Wang, G. H. Robinson, *Inorg. Chem.* **2011**, *50*, 12326–12337; b) J. B. Waters, T. A. Everitt, W. K. Myers, J. M. Goicoechea, *Chem. Sci.* **2016**, *7*, 6981–6987.
[32] G. M. Sheldrick, *Acta Crystallogr.* **2015**, *C71*, 3–8.
[33] Gaussian 16, Revision C.01, M. J. Frisch, G. W. Trucks, H. B. Schlegel, G. E. Scuseria, M. A. Robb, J. R. Cheeseman, G. Scalmani, V. Barone, G. A. Petersson, H. Nakatsuji, X. Li, M. Caricato, A. V. Marenich, J. Bloino, B. G. Janesko, R. Gomperts, B. Mennucci, H. P. Hratchian, J. V. Ortiz, A. F. Izmaylov, J. L. Sonnenberg, D. Williams-Young, F. Ding, F. Lipparini, F. Egidi, J. Goings, B. Peng, A. Petrone, T. Henderson, D. Ranasinghe, V. G. Zakrzewski, J. Gao, N. Rega, G. Zheng, W. Liang, M. Hada, M. Ehara, K. Toyota, R. Fukuda, J. Hasegawa, M. Ishida, T. Nakajima, Y. Honda, O. Kitao, H. Nakai, T. Vreven, K. Throssell, J. A. Montgomery, Jr., J. E. Peralta, F. Ogliaro, M. J. Bearpark, J. J. Heyd, E. N. Brothers, K. N. Kudin, V. N. Staroverov, T. A. Keith, R. Kobayashi, J. Normand, K. Raghavachari, A. P. Rendell, J. C. Burant, S. S. Iyengar, J. Tomasi, M. Cossi, J. M. Millam, M. Klene, C. Adamo, R. Cammi, J. W. Ochterski, R. L. Martin, K. Morokuma, O. Farkas, J. B. Foresman, D. J. Fox, Gaussian, Inc., Wallingford CT, 2016.
[34] A. D. Becke, *J. Chem. Phys.* **1993**, *98*, 5648–5652.
[35] S. Grimme, S. Ehrlich, L. Goerigk, *J. Comb. Chem.* **2011**, *32*, 1456–1465.
[36] F. Weigend, R. Ahlrichs, *Phys. Chem. Chem. Phys.* **2005**, *7*, 3297–3305.
[37] G. Schaftenaar, J. H. Noordik, *J. Comput.-Aided Mol. Des.* **2000**, *14*, 123–132.

Manuscript received: November 30, 2021
Revised manuscript received: December 17, 2021
Accepted manuscript online: December 20, 2021